Journal of Chromatography A, 1217 (2010) 2254–2261

Contents lists available at ScienceDirect

Journal of Chromatography A

journal homepage: www.elsevier.com/locate/chroma

# Quantitative study of stereospecific binding of monoclonal antibody to *anti*-benzo(a)pyrene diol epoxide-$N^2$-dG adducts by capillary electrophoresis immunoassay

Chao Wang, Tao Li, Zhixin Wang, Feng Feng, Hailin Wang*

*State Key Laboratory of Environmental Chemistry and Eco-toxicology, Research Center for Eco-Environmental Sciences, Chinese Academy of Sciences, Shuangqing Road 18, Haidian Distr., Beijing 100085, China*

ARTICLE INFO

*Article history:*
Received 16 October 2009
Received in revised form 3 February 2010
Accepted 12 February 2010
Available online 20 February 2010

*Keywords:*
Stereochemistry
Capillary electrophoresis
Immunoassays
Benzo[a]pyrene
DNA adducts

ABSTRACT

The stereospecific binding of monoclonal antibody (mAb) 8E11 to *anti*-benzo(a)pyrene diol epoxide (BPDE)-dG adducts in single nucleoside, long oligonucleotide, and genomic DNA were quantitatively evaluated using noncompetitive and competitive capillary electrophoresis (CE) immunoassays. Two single-stranded TMR-BPDE-90mers containing a single *anti*-BPDE-dG adduct with defined stereochemistry and a fluorescent label at 5′-end were used as fluorescent probes for competitive CE immunoassay. To quantitatively evaluate the binding affinity through competitive CE immunoassays, a series of equations were derived according to the binding stoichiometry. The binding of mAb 8E11 to *trans*-(+)-*anti*-BPDE-dG displays strongest affinity ($K_b$: $3.57 \times 10^8$ $M^{-1}$) among all four investigated *anti*-BPDE-dG mononucleoside adducts, and the *cis*-(−)-*anti*-BPDE-dG displays lowest affinity ($K_b$: $1.14 \times 10^7$ $M^{-1}$). The binding of monoclonal antibody (mAb) 8E11 to BPDE-dG adducts in long DNA (90mer) preferentially forms the complex with a stoichiometry of 1:1, and that mAb 8E11 displays a slightly higher affinity with *trans*-(+)-*anti*-BPDE-90mers ($K_b$: $6.36 \pm 0.54 \times 10^8$ $M^{-1}$) than *trans*-(−)-*anti*-BPDE-90mers ($K_b$: $4.52 \pm 0.52 \times 10^8$ $M^{-1}$). The mAb 8E11 also displays high affinity with BPDE-dG adducts in genomic DNA ($K_b$: $3.74 \times 10^8$ $M^{-1}$), indicating its promising applications for sensitive immuno-detection of BPDE-DNA adducts in genomic DNA.


## 1. Introduction

Specific binding of antibody to antigen or hapten dictates the applications of immunoassays [1]. Qualitative and quantitative study of such binding is essential not only to the understanding of the molecular basis for immune functions, and also important to the method development of immunoassays. Various techniques have been developed for binding study, such as enzyme-linked immunosorbent assay (ELISA) [2–4], surface plasmon resonance (SPR) [5–7], gel electrophoresis mobility shift assay (EMSA) [8,9], and affinity chromatography [10,11]. Most immunoassays heavily rely on the adsorption of antigen or antibody on solid/liquid surface, e.g. ELISA, however, such adsorption can significantly alter the binding activity of the reactant (e.g. partially denaturing antibodies), and cause a decrease in binding capacity of the antigen-antibody [12]. Moreover, solid phase based immunoassays only provide limited binding information. For example, it is hard for ELISA to distinguish the complexes with different binding stoichiometry through the involved sequential washing.

Capillary electrophoresis (CE) immunoassay is a solution based affinity technique, and can provide accurate aqueous solution related binding information on affinity and stoichiometry [13,14]. In typical CE immunoassays, the initial concentration of antigen/hapten or antibody is known, and the bound and unbound species can be measured. Moreover, due to high efficiency of the CE separation, antigen–antibody complexes with different binding stoichiometry may be separated from each other. In addition, with combined laser-induced fluorescence detection (LIF), the CE immunoassay has demonstrated a number of advantages, e.g. high sensitivity, rapid separation, minute amount of analyte consumed, and ease-of-automation [15,16].

Both noncompetitive and competitive immunoassays have been employed in CE-LIF immunoassay [17,18]. In typical noncompetitive CE-LIF immunoassays, a known amount of fluorophore-labeled antibody (Ab*) is mixed with antigen (Ag) to form detectable noncovalent Ab*–Ag immunocomplex. The formed Ab*–Ag complex and unbound Ab* can be separated by highly efficient CE and detected by coupled highly sensitive LIF. Both Ab*–Ag complex and free Ab* can be measured, and both the measured signals can be used for accurate quantification of target antigen. Noncom-

* Corresponding author. Tel.: +86 10 62849600; fax: +86 10 62849600.
*E-mail address:* hlwang@rcees.ac.cn (H. Wang).

0021-9673/$ – see front matter © 2010 Elsevier B.V. All rights reserved.
doi:10.1016/j.chroma.2010.02.024

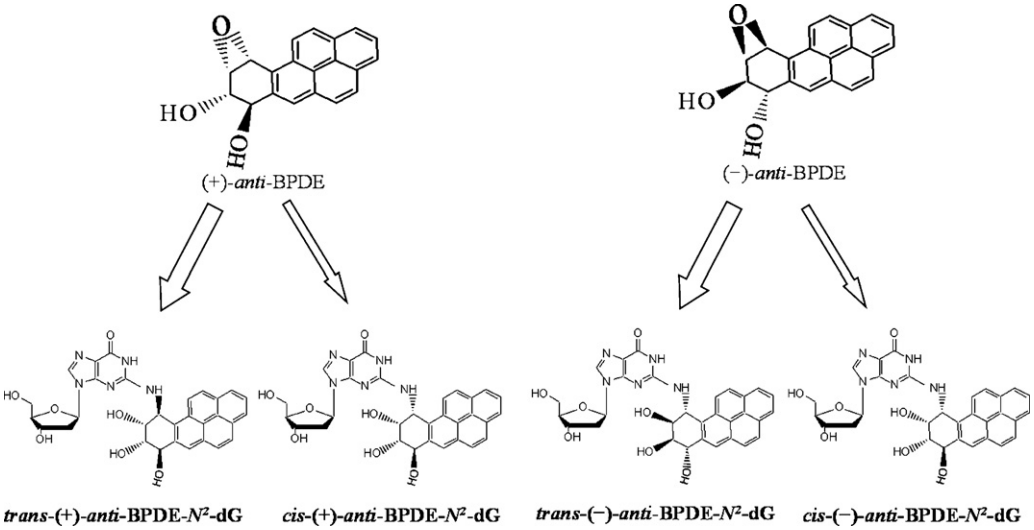


**Fig. 1.** Structure of *anti*-BPDE enantiomers (top) and corresponding four *anti*-BPDE-$N^2$-dG stereomers (bottom).

petitive immunoassays have several remarkable advantages over competitive immunoassays, including wider dynamic range and lower detection limits [19]. However, noncompetitive immunoassays require appropriate label of the antibody, which may scarify the binding avidity of the antibody. Competitive immunoassays may provide alternative choice. In this case, a fluorescently labeled antigen analog (Ag*) was used instead. This approach is based on the competition of Ag and Ag* for the limited binding sites of Ab. CE-LIF analysis of the mixture presents two types of separated zones corresponding to Ag* and Ag*–Ab. The binding affinity of Ab and unlabeled Ag can be indirectly derived from the signal change of Ag* and Ag*–Ab complex shown in the CE-LIF analysis.

Benzo[a]pyrene, an extensively studied carcinogenic polycyclic aromatic hydrocarbons (PAHs) [20], can be stereoselectively metabolized *in vivo* by cytochrome P450 and epoxide hydrolase to form two stereoisomic benzo[a]pyrene-7,8-diol-9,10-epoxide ((±)-*anti/syn*-BPDE) [21]. (±)-*anti*-BPDE is more mutagenic than the diastereomer (±)-*syn*-BPDE in a series of animal and human cell experiments [22,23]. Even the mutagenesis of two *anti*-BPDE enantiomers in bacterial and mammalian cells may be different [24–28]. The reactive carcinogenic species (±)-*anti*-BPDE can react with DNA, primarily at the exocyclic $N^2$ amino group of deoxyguanosine (dG) to form a bulky adduct of *anti*-BPDE-$N^2$-dG with four stereoisomers, including (+)-*trans*, (−)-*trans*, (+)-*cis*, and (−)-*cis* (Fig. 1). The stereochemistry of the four *anti*-BPDE-$N^2$-dG adducts has been proved to determine their respective mutagenesis and carcinogensis [29–34]. A number of antisera have been produced for developing sensitive and specific immunoassay of BPDE-DNA adducts (Table 1) [35–40]. These antibodies exhibit varied affinity, stereoselectivity, and specificity. The affinity is usually evaluated by the concentration of 50% inhibition ($IC_{50}$) through competitive ELISA assay, which depends upon the concentration of the antibody and labeled antigen. Concentration-independent binding information often lacks. Among these antibodies, mAb 8E11 has been screened in our laboratory as an important diagnostic monoclonal antibody and often used in the detection of BPDE-DNA adducts [18,35,36,41–43]. However, the relevant information on affinity, stereoselectivity, and specificity has not been clarified yet.

In this work, we developed CE immunoassay methods for quantitative study of the binding of BPDE-dG DNA adducts to mAb 8E11, which is useful for human exposure biomonitoring of carcinogenic benzo(a)pyrene. A series of equation were derived and examined by CE immunoassays for quantitative affinity study. Based on derived equations and CE immunoassays study, the binding affinity, stoichiometry, specificity, and stereoselectivity of mAb 8E11 against BPDE-dGs, BPDE-90mers and BPDE genomic DNA were examined.

## 2. Theoretical section

### 2.1. 1:1 noncompetitive binding stoichiometry

A series of equations were derived to calculate binding parameters for IgG antibody P and large antigen A, which was labeled with fluorophore in immunoassays. First, it is assumed that P binds with A at 1:1 stoichiometry. This is true when the antigen is very large and the first binding of the antigen may induce steric barrier to the second binding to the bivalent IgG. The reaction between A and P

**Table 1**
Antisera developed against BPDE-DNA adduct.

| Antibody | Animal | Immunogen | Isotype | Cross-reactivity |
|---|---|---|---|---|
| mAb 8E11 [35,36] | Balb/cCr mice | BPDE-I-G-BSA | IgG1, Kappa | No |
| mAb E5 [36,40] | Balb/cCr mice | BPDE-I-G-BSA | unknown | No |
| mAb 5D11 [35,36] | Balb/cCr mice | BPDE-I-DNA-MBSA | IgG2, Kappa | Yes |
| mAb 41D3 [39] | Balb/cCr mice | BPDE-I-DNA-MBSA | unknown | Yes |
| mAb 5D2 [37,38] | Balb/cCr mice | BPDE-I-DNA-MBSA | IgG1, Kappa | Unknown |
| mAb 1D7 [37] | Balb/cCr mice | BPDE-I-DNA-MBSA | IgG1, Kappa | Unknown |
| mAb 4C2 [37] | Balb/cCr mice | BPDE-I-DNA-MBSA | IgG1, Kappa | Unknown |
| mAb TNO [39] | Balb/cCr mice | BPDE-I-DNA-MBSA | Unknown | Unknown |
| pAb #29 [37] | New Zealand white rabbits | BPDE-I-modified DNA | Unknown | Yes |
| pAb BP1 [38] | New Zealand white rabbits | BPDE-I-modified DNA | Unknown | Yes |
| pAb F29, F30, NCI [39] | New Zealand white rabbits | BPDE-I-DNA-MBSA | Unknown | Yes |

mAb and pAb refer to monoclonal antibody and polyclonal antibody, respectively.

can be described as below:

$$A + P \xrightarrow{K_b} AP$$

Equilibrium equation can be expressed as follows:

$$K_b = \frac{[AP]}{[A][P]} \quad (1\text{-}1)$$

The terms [A] and [P] represent the free concentration of A and P while [AP] is the bound concentration of A to P. $k$ is defined as the ratio of the concentration of AP to total concentration of A in the Eq. (1-2).

$$k = \frac{[AP]}{[A]_t} \quad (1\text{-}2)$$

The subscript $t$ in all equations denotes total concentration of corresponding species in the solution. Expressions for $[P]_t$ and $[A]_t$ can be obtained according to the mass action law.

$$[P]_t = [P] + [AP] \quad (1\text{-}3)$$

$$[A]_t = [AP] + [A] \quad (1\text{-}4)$$

By substituting [AP] from Eq. (1-2) into Eqs. (1-3) and (1-4), Eqs. (1-5) and (1-6) can be obtained:

$$[P] = [P]_t - k[A]_t \quad (1\text{-}5)$$

$$[A] = [A]_t(1 - k) \quad (1\text{-}6)$$

By substituting [P], [A], [AP] from Eqs. (1-5), (1-6) and (1-2) into Eq. (1-1), Eq. (1-7) can be obtained:

$$K_b = \frac{k}{(1 - k)([P]_t - k[A]_t)} \quad (1\text{-}7)$$

In noncompetitive immunoassays, the binding constant for antibody P and antigen A can be calculated by Eq. (1-7).

### 2.2. 1:1 and 1:1 competitive binding stoichiometry

We derived a series of equations for simple competitive immunoassays. A is large antigen labeled with fluorophore. B is an unlabeled big antigen. A and B are assumed to bind to only one binding site of IgG antibody P at 1:1 stoichiometry. The binding constant $K_b$ of A to P can be obtained by noncompetitive immunoassays with Eq. (1-7).

For A, B, and P in aqueous solution, there are two binding reactions:

$$A + P \xrightarrow{K_b} AP$$
$$B + P \xrightarrow{K_1} BP$$

Their equilibrium equations can be expressed as follows:

$$K_b = \frac{[AP]}{[A][P]} \quad (2\text{-}1)$$

$$K_1 = \frac{[BP]}{[B][P]} \quad (2\text{-}2)$$

$k$ is defined as follows, which can be calculated by the concentrations of AP and A.

$$k = \frac{[AP]}{[A]_t} = \frac{[AP]}{[A] + [AP]} \quad (2\text{-}3)$$

Eq. (2-3) shows that $k$ represents the binding rate of antigen A with antibody P. From Eq. (2-3), Eq. (2-4) can be obtained:

$$\frac{[AP]}{[A]} = \frac{k}{1 - k} \quad (2\text{-}4)$$

From Eq. (2-2), Eq. (2-5) can be obtained as follows:

$$[B] = \frac{[BP]}{K_1[P]} \quad (2\text{-}5)$$

M is defined as follows:

$$M = \frac{(1 - k)K_b}{k} \quad (2\text{-}6)$$

By substituting [AP]/[A] from Eq. (2-4) into Eq. (2-1), Eq. (2-7) can be obtained:

$$[P] = \frac{k}{K_b(1 - k)} = \frac{1}{M} \quad (2\text{-}7)$$

Eq. (2-7) shows that M is the reciprocal of free antibody [P].

Expressions for $[P]_t$ and $[B]_t$ can be obtained according to the mass action law.

$$[P]_t = [AP] + [P] + [BP] \quad (2\text{-}8)$$

$$[B]_t = [B] + [BP] \quad (2\text{-}9)$$

By substituting [AP] and [P] from Eqs. (2-3) and (2-7) into Eq. (2-8), Eq. (2-10) can be obtained:

$$[BP] = [P]_t - \frac{1}{M} - k[A]_t \quad (2\text{-}10)$$

By dividing [BP] (ref. to Eq. (2-10)) by [P] (ref. to Eq. (2-7)), Eq. (2-11) can be obtained:

$$\frac{[BP]}{[P]} = M[P]_t - kM[A]_t - 1 \quad (2\text{-}11)$$

By substituting [BP]/[P] from Eq. (2-11) into Eq. (2-5), Eq. (2-12) can be obtained:

$$[B] = \frac{1}{K_1}(M[P]_t - kM[A]_t - 1) \quad (2\text{-}12)$$

By substituting [BP] and [B] from Eqs. (2-10) and (2-12) into Eq. (2-9), Eq. (2-13) can be obtained:

$$(M[P]_t - kM[A]_t - 1) = K_1\left([B]_t - [P]_t + k[A]_t + \frac{1}{M}\right) \quad (2\text{-}13)$$

By substituting $M$ with Eq. (2-7) and $k$ with Eq. (2-3) back into Eq. (2-13), Eq. (2-14) can be obtained:

$$K_b\left(\frac{[P]_t}{[AP]} - 1\right)[A] = (1 - K_1[P]_t) + K_1\left([B]_t + [AP] + \frac{[AP]}{K_b[A]}\right) \quad (2\text{-}14)$$

We defined $X$ and $Y$ as follows to linear $K_1$ in charts:

$$X = [B]_t + [AP] + \frac{[AP]}{K_b[A]} \quad (2\text{-}15)$$

$$Y = K_b\left(\frac{[P]_t}{[AP]} - 1\right)[A] \quad (2\text{-}16)$$

By substituting $M = (1 - k)K_b/k$ and $k$ from Eq. (2-3) back into Eq. (2-13), a simple equilibrium equation can be obtained again:

$$\frac{[BP]}{[P]} = K_1[B] \quad (2\text{-}17)$$

The Eq. (2-17) shows that the derived Eq. (2-14) is consistent with the definition of binding constant of B and P, as shown in the Eq. (2-2).

### 2.3. 1:1 and 2:1 competitive binding stoichiometry

We also derived a series of equations to calculate binding constants for antibody and small antigens in competitive immunoassays. P, antibody, has two binding sites: $P_1$ and $P_2$. In order for clear derivation, we separate P into two parts: $P_1$ and $P_2$. So the total concentration of P, $P_1$ and $P_2$ is equal to each other. There are several assumptions. A, big antigen labeled with fluorophore,

could bind only to $P_1$ site. B, small antigen without fluorophore label, could bind independently to both $P_1$ and $P_2$ site with the same binding constant. The binding of A to $P_1$ does not interfere with that of B to $P_2$.

For A, B, $P_1$ and $P_2$ in aqueous solution, there are three binding reactions:

$$A + P_1 \xrightarrow{K_b} AP_1$$
$$B + P_1 \xrightarrow{K_1} BP_1$$
$$B + P_2 \xrightarrow{K_2} BP_2$$

$AP_1$, $BP_1$ and $BP_2$ represent the complexes of A, B with $P_1$ and the complex of B with $P_2$, respectively. The equilibrium equations can be expressed as follows:

$$K_b = \frac{[AP_1]}{[A][P_1]} \tag{3-1}$$

$$K_1 = \frac{[BP_1]}{[B][P_1]} \tag{3-2}$$

$$K_2 = \frac{[BP_2]}{[B][P_2]} \tag{3-3}$$

In the Eqs. (3-1), (3-2) and (3-3), $K_b$, $K_1$ and $K_2$ and are the binding constants for binding of A to $P_1$, B to $P_1$ and $P_2$, respectively. $K_b$ can be determined by previous noncompetitive immunoassay. The terms [A], [B], [$P_1$] and [$P_2$] represent the free concentration of A, B, $P_1$ and $P_2$ while [$AP_1$], [$BP_1$] and [$BP_2$] are the bound concentration of A to $P_1$, B to $P_1$ and $P_2$. The subscript $t$ in the following equations denotes total concentration of corresponding species in the solution. $k$ is defined as follows, which can be calculated by area of peaks $AP_1$ and A in CE analysis.

$$k = \frac{[AP_1]}{[A]_t} = \frac{[AP_1]}{[A] + [AP_1]} \tag{3-4}$$

From Eq. (3-4), Eq. (3-5) can be obtained:

$$\frac{[AP_1]}{[A]} = \frac{k}{1-k} \tag{3-5}$$

From Eq. (3-2), Eq. (3-6) can be obtained as follows:

$$[B] = \frac{[BP_1]}{K_1[P_1]} \tag{3-6}$$

$M$ is defined as Eq. (2-6):

$$M = \frac{(1-k)K_b}{k}$$

By substituting [$AP_1$]/[A] from Eq. (3-5) into Eq. (3-1), Eq. (3-7) can be obtained:

$$[P_1] = \frac{k}{K_b(1-k)} = \frac{1}{M} \tag{3-7}$$

Expressions for $[P_1]_t$, $[P_2]_t$ and $[A]_t$ can be obtained according to the mass action law.

$$[P_1]_t = [BP_1] + [P_1] + [AP_1] \tag{3-8}$$

$$[P_2]_t = [BP_2] + [P_2] \tag{3-9}$$

$$[B]_t = [B] + [BP_1] + [BP_2] \tag{3-10}$$

By substituting [$AP_1$] and [$P_1$] from Eqs. (3-4) and (3-7) into Eq. (3-8), Eq. (3-11) can be obtained:

$$[BP_1] = [P]_t - \frac{1}{M} - k[A]_t \tag{3-11}$$

By dividing Eq. (3-11) to Eq. (3-7), Eq. (3-12) can be obtained:

$$\frac{[BP_1]}{[P_1]} = M[P]_t - kM[A]_t - 1 \tag{3-12}$$

As B binds independently to $P_1$ and $P_2$, the binding constants $K_1$ and $K_2$ are equal to each other. So substituting [B] from Eq. (3-6) and [$P_2$] from Eq. (3-9) into Eq. (3-3), Eq. (3-13) can be obtained:

$$[BP_2] = \frac{([BP_1]/[P_1])[P]_t}{[BP_1]/[P_1] + 1} \tag{3-13}$$

By substituting [$BP_1$]/[$P_1$] from Eq. (3-12) into Eqs. (3-6) and (3-13), Eqs. (3-14) and (3-15) can be obtained:

$$[B] = \frac{1}{K_1}(M[P]_t - kM[A]_t - 1) \tag{3-14}$$

$$[BP_2] = [P]_t - \frac{[P]_t}{M[P]_t - kM[A]_t} \tag{3-15}$$

By substituting [$BP_1$], [B] and [$BP_2$] from Eqs. (3-11), (3-14) and (3-15) into Eq. (3-10), Eq. (3-16) can be obtained:

$$(M[P]_t - kM[A]_t - 1) = K_1\left([B]_t - 2[P]_t + k[A]_t + \frac{1}{M} + \frac{[P]_t}{M([P]_t - k[A]_t)}\right) \tag{3-16}$$

By substituting $M$ with Eq. (3-7) and $k$ with Eq. (3-4) back into Eq. (3-16), Eq. (3-17) can be obtained:

$$K_b\left(\frac{[P]_t}{[AP_1]} - 1\right)[A] = (1 - 2K_1[P]_t) + K_1\left([B]_t + [AP_1] + \frac{[AP_1]}{K_b[A]} \times \frac{2[P]_t - [AP_1]}{[P]_t - [AP_1]}\right) \tag{3-17}$$

We defined $X$ and $Y$ as follows to linear $K_1$ in charts:

$$X = [B]_t + [AP_1] + \frac{[AP_1]}{K_b[A]} \times \frac{2[P]_t - [AP_1]}{[P]_t - [AP_1]} \tag{3-18}$$

$$Y = K_b\left(\frac{[P]_t}{[AP_1]} - 1\right)[A] \tag{3-19}$$

By substituting $M = (1-k)K_b/k$ and $k$ from Eq. (3-4) back into Eq. (3-17), a simple equation can be obtained:

$$\frac{[BP_1]}{[P_1]} = K_1[B] \tag{3-20}$$

The Eq. (3-20) shows that Eq. (3-17) is consistent with the definition of binding constant of B and $P_1$, as shown in the Eq. (3-2).

## 3. Materials and methods

### 3.1. Chemicals and reagents

All the tetramethylrhodamine (TMR)-labeled and unmodified oligonucleotides were synthesized by TaKaRa Biotech (Dalian, China). (±)-*r*-7,*t*-8-dihydroxy-*t*-9,10-epoxy-7,8,9,10-tetrahydro benzo[a]pyrene [(±)-*anti*-BPDE] was purchased from the National Cancer Institute Chemical Carcinogen Reference Standard Repository, Midwest Research Institute (Kansas City, MO, USA). Monoclonal mouse *anti*-BPDE antibody IgG 8E11 (mAb 8E11) was purchased from Trevigen (Gaithersburg, MD, USA). Bovine serum albumin (BSA) was obtained from Sigma–Aldrich (St. Louis, MO, USA). Tris-(hydroxymethyl)-aminomethane (Tris) and glycine were purchased from Amresco (Solon, OH, USA). Other chemicals were supplied by Sigma-Aldrich (St. Louis, MO, USA) or Fisher Scientific (Pittsburgh, PA, USA).

### 3.2. Preparation of stereoisomeric BPDE-90mers, BPDE-dGs and BPDE adducted genomic DNA

Single-stranded BPDE-90mer probes (TMR-BPDE-ss90mers) were synthesized according to our previous work [44]. The probes contain a fluorescent label at 5′ termini and a single *anti*-BPDE-$N^2$-dG adduct with defined stereochemistry in the middle of the chain. Briefly, a 16mer of 5′-CCCATTATGCATAACC-3′ was incubated with racemic (±)-*anti*-BPDE to synthesize BPDE-16mer adducts. The incorporation of BPDE in the reacted 16mers was validated by HPLC retention, UV spectroscopy, and HPLC-Q-TOF-MS analysis, and the stereochemistry of the BPDE adducts was further identified by enzyme digestion into single nucleoside adducts in combination with well-established HPLC-diode array detection (DAD)-fluorescence detection (FL) stereoselective analysis of four optically active BPDE-$N^2$-gunaines. Then BPDE-16mers were ligated with the other 2 oligonucleotides for synthesis of TMR-BPDE-ss90mers followed by purification with 8% denaturing polyacrylamide gel electrophoresis (PAGE). The final TMR-BPDE-ss90mers were quantified by UV absorbance at 260 nm. Unlabeled BPDE-ss90mers were prepared with same protocol except that the gel was required to be stained by ethidium bromide for visualization.

Four stereoisomers of *anti*-BPDE-$N^2$-dG mononucleoside adduct were prepared as described recently [45]. The synthesis started with a direct reaction of racemic (±)-*anti*-BPDE with dG, followed by optimized solid-phase extraction (SPE) and HPLC purification. Four BPDE-dG stereoisomers were characterized by LC-UV-MS, LC-DAD-FL, circular dichroism (CD), and finally quantified by UV absorbance at 260 nm [45].

*anti*-BPDE adducted genomic DNA was synthesized by the direct reaction of racemic *anti*-BPDE with genomic DNA. Approximately 2 mg genomic DNA extracted from cultured A549 human lung carcinoma cells was dissolved in 200 μL 100 mM Tris–HCl buffer (pH 7.5), and (±)-*anti*-BPDE (5 μL, dissolved in fresh 19:1 (v/v) tetrahydrofuran/triethylamine solution) was added with a final concentration of 1 μM. The mixture was incubated under gentle shake at room temperature over 16 h in dark. Then the reacted DNA was precipitated, air-dried, and re-dissolved for further analyses. The DNA concentration was measured by UV absorbance at 260 nm and the concentration of BPDE adduct was quantified by the process of enzyme digestion and UPLC–MS analysis, as described in our recent work [46].

### 3.3. Capillary electrophoresis with laser-induced fluorescence

CE analysis was carried out using a laboratory-built CE-LIF system as described previously [47]. Briefly, Electrophoresis was driven using a high voltage power supply (Tianjin Dongwen High-Voltage Power Supply Plant, Tianjin, China). A green He–Ne laser beam (543.5 nm, 1 mW, Melles Griot, Irvine, CA, USA) with an excitation wavelength of 543.5 nm was focused by a 6.3 × (N.A. 0.20) microscope objective (Melles Griot, Irvine, CA, USA) on the capillary detection window. The excited fluorescence was spectrally filtered with a band-pass of 575 nm (Semrock, Rochester, NY, USA) and detected by a photomultiplier tube (PMT, Model R3896, Hamamatsu Photonics, Japan). The PMT signal was transferred to the current-to-voltage converter and digitized by HW-2000 chromatographic workstation (Qianpu Software Co., Shanghai, China) with a data acquisition frequency of 20 Hz. Uncoated fused silica capillary was purchased from Yongnian Optical Fiber Company (Hebei, China) with a dimension of 25 μm i.d. × 365 μm o.d. and 36 cm long (effective length, 29 cm) throughout the experiments. Prior to use, the new capillary was rinsed with methanol (30 min), 0.1 M NaOH (120 min), purified water (10 min), and finally running buffer (120 min) and was conditioned with running buffer overnight.

Samples were electrokinetically injected into the capillary by applying an injection voltage of 15 kV for 5 s. The separation was carried out by applying a voltage of 15 kV at room temperature. The sample and running buffers were 2× Tris–glycine–acetic acid buffer (TGA, pH 7.5, 14 mM Tris, 108 mM Glycine, HAc ~10.5 mM) and 1× Tris–glycine buffer (TG, pH 8.5, 30 mM Tris, 160 mM Glycine), respectively. Each sample was repeatedly injected for three times. Every three runs, the capillary was washed with 0.02 M NaOH electrophoretically at 15 kV for 4 min followed by electrophoresis using water (1 min) and running buffer (5 min).

### 3.4. Capillary electrophoresis immunoassays of BPDE-DNA adducts with mAb 8E11

In noncompetitive immunoassays, TMR-BPDE-ss90mer probes were diluted to appropriate concentration in sample buffer 2 × TGA. For experiments involving antibody, antibody stock solutions were diluted in sample buffer 2 × TGA immediately before analysis and kept on ice. After addition of BSA, TMR and antibody, the sample was given gently vortex to ensure complete mixing and incubated at 37 °C for 30 min before CE-LIF analysis. In all immunoassays, TMR was used as an internal standard to correct variations in the injection volume, and BSA was used to enhance the formation and stability of the immuno-complexes [48]. Sample buffer 2 × TGA and running buffer 1 × TG were selected to perform transient anion isotachophoresis (t-ITP) to increase the sensitivity of detection [16].

In the competitive immunoassays with the competitors of BPDE-dGs, BPDE-90mers or BPDE genomic DNA, the competitors were diluted to different concentrations in sample buffer 2 × TGA. Then TMR-BPDE-ss90mer probes, BSA, TMR and mAb 8E11, were added to the mixture in turn. After gently vortex, the mixture was incubated at 37 °C for 30 min and eventually subjected to CE-LIF analysis to detect both antibody-bound and unbound fluorescent probes. Prior to competitive immunoassays with BPDE genomic DNA, an aliquot of BPDE adducted genomic DNA was denatured at 95 °C for 10 min, followed by cooling on ice.

## 4. Results and discussion

### 4.1. Noncompetitive immunoassays between TMR-BPDE-ss90mer and mAb 8E11

The binding stoichiometry of two stereoisomeric BPDE-90mer probes, *trans*-(−)-*anti*-BPDE-90mer probe (*trans*(−) probe) and *trans*-(+)-*anti*-BPDE-90mer probe (*trans*(+) probe), and mAb 8E11 was studied by noncompetitive immunoassays, as shown in Fig. 2. One extra peak of complex (peak 2, ~2.46 min) is observed before the elution of free probe (peak 1, ~2.53 min) once mAb 8E11 is added into the probe solution. Moreover, only one predominant immunocomplex peak was detected for both BPDE-90mer probes even with the varied ratio of mAb 8E11 to the probes (Fig. 2). Previous study shows that mAb 8E11 can form binary (1:1) and tertiary (1:2) complex with two BPDE adducts in a short oligonucleotide (16mer) in a concentration-dependent manner [18]. In this study, the longer strand (90mer) and more negative charge of the BPDE-90mer probes may provide steric barrier and electrostatic exclusion and is adverse to the formation of tertiary immunocomplex (1:2). Therefore, most of the BPDE-90mer probe is bound to mAb 8E11 at 1:1 stoichiometry regardless of the ratio of mAb 8E11 to the probes. The results may suggest that mAb 8E11 binding to the BPDE adducts in long DNA predominantly in the stoichiometry of 1:1.

In Fig. 3, different concentration of BPDE-90mer probe (0.0125~5 nM) was used to bind with mAb 8E11 at a fixed con-

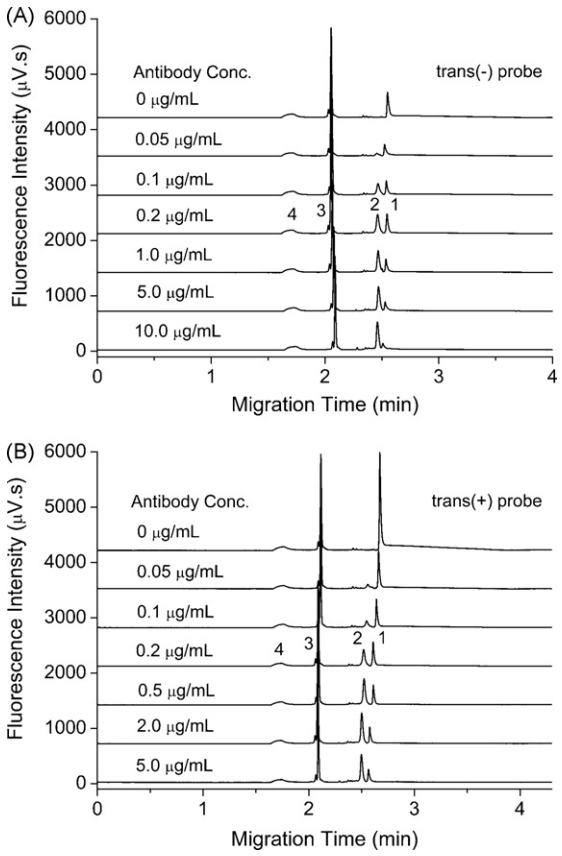


**Fig. 2.** Electropherograms from capillary electrophoresis analysis of mixture containing two stereoisomeric BPDE-90mers (A: *trans*(−) probe, B: *trans*(+) probe) and varying concentration of mAb 8E11. The concentration of antibody ranged from 0 to 10 μg/mL while the concentration of two TMR-BPDE-90mer probes was fixed at 5 nM. Peak 1, 2, 3 and 4 corresponded to single-stranded 90mer probe, complex of 90mer probe and mAb 8E11, TMR and the impurity of TMR.

centration of 0.5 μg/mL. It shows the binding percentage of two stereoisomeric fluorescent probes is a function of the probe concentration, decreasing with the increasing concentration of the probes. Because of their binding stoichiometry of 1:1, the binding constants of mAb 8E11 and BPDE-90mer probes were estimated by the 1:1 stoichiometry based equilibrium Eq. (1-7). The calculated binding constants are $4.52 \pm 0.52 \times 10^8$ $M^{-1}$ for *trans*(−) probe and $6.36 \pm 0.54 \times 10^8$ $M^{-1}$ for *trans*(+) probe, respectively. The results indicate that mAb 8E11 has a slightly higher affinity for *trans*-(+)-*anti*-BPDE-$N^2$-dG adduct in oligonucleotides than that

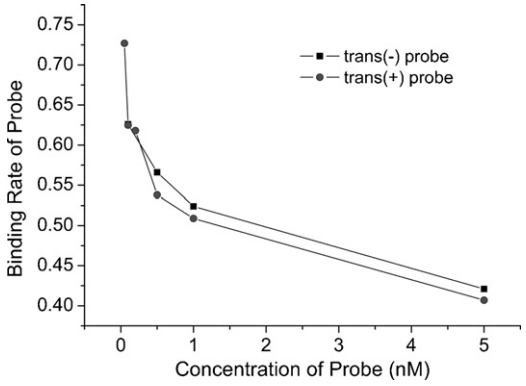


**Fig. 3.** Comparison of binding percentage of two stereoisomers of TMR-BPDE-90mer probes with mAb 8E11. The concentration of the probes ranged from 0.05 to 5 nM while the concentration of mAb 8E11 was fixed at 0.5 μg/ml.

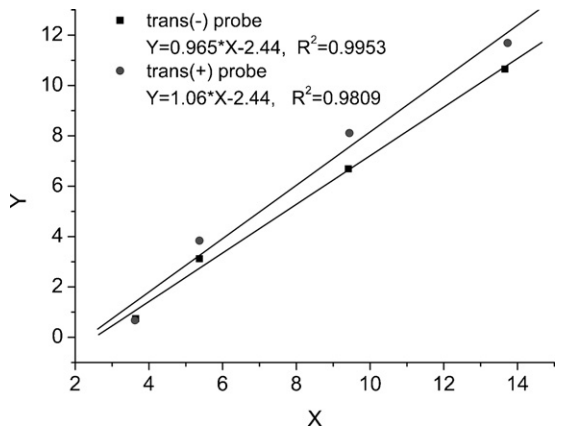


**Fig. 4.** Linear regression analysis from competitive immunoassays of *trans*-(+)-BPDE-90mer and two TMR-BPDE-ss90mer probes with mAb 8E11 by Eq. (2-14). Axes *X* and *Y* are defined by Eqs. (2-15) and (2-16), respectively. The concentration of unlabeled *trans*-(+)-BPDE-90mer ranged from 1.8 to 13.3 nM while the concentrations of mAb 8E11 and TMR-BPDE-ss90mer probe were fixed at about 0.25 μg/ml and 5 nM, respectively.

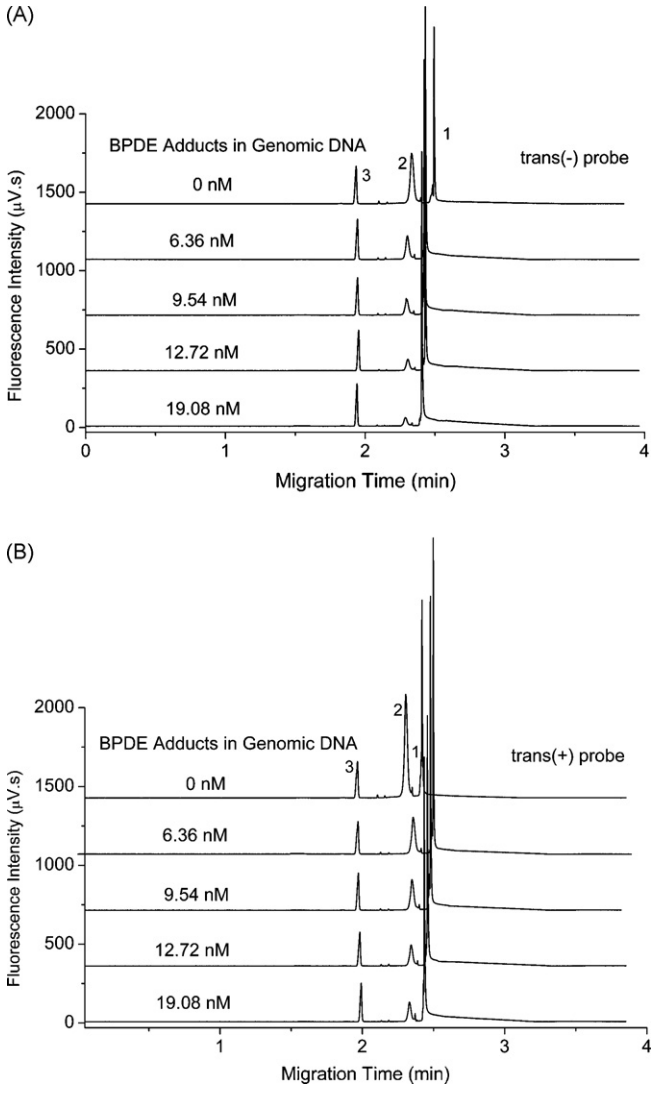


**Fig. 5.** Electropherograms from CE-LIF competitive immunoassays of two TMR-BPDE-ss90mer probes (A: *trans*(−) probe, B: *trans*(+) probe) and BPDE genomic DNA with mAb 8E11. The BPDE adduct concentration of genomic DNA ranged from 0 to 19.08 nM while the concentrations of mAb 8E11 and TMR-BPDE-ss90mer probe were fixed at about 0.25 μg/ml and 5 nM, respectively. Peak 1, 2 and 3 corresponded to single-stranded 90mer probe, complex of 90mer probe and antibody 8E11, and TMR.

for *trans*-(−)-*anti*-BPDE-$N^2$-dG adduct. These results are consistent with previous work [37].

### 4.2. Competitive immunoassays between TMR-BPDE-ss90mer and BPDE genomic DNA adduct with mAb 8E11

To study the binding of the BPDE-$N^2$-dG adduct in fluorescently unlabeled genomic DNA and single nucleoside to mAb 8E11, competitive immunoassays were further developed by using TMR-BPDE-ss90mer probes. First, Eq. (2-14) that was derived for the competitive binding stoichiometry of 1:1 is appropriate to study the binding of mAb 8E11 to the BPDE adducts in long DNA. To validate this equation, we examined the binding of mAb 8E11 to fluorescently unlabeled *trans*-(+)-BPDE-90mer through competitive immunoassays in which two stereochemically different TMR-BPDE-ss90mer were used as affinity probes, respectively. Fig. 4 shows the obtained linear regression curves of the two competitive immunoassays: $Y = 0.965 \times X - 2.44$ ($R^2 = 0.9953$) for *trans*(−) probe and $Y = 1.06 \times X - 2.44$ ($R^2 = 0.9809$) for *trans*(+) probe. As the estimated slope value equals the value of the binding constant (see Eq. (2-14)), the obtained binding constants for *trans*(+) BPDE-90mer and mAb 8E11 were estimated as $9.65 \pm 0.47 \times 10^8\ M^{-1}$ and $1.06 \pm 0.10 \times 10^9\ M^{-1}$ when *trans*(−) and *trans*(+)TMR-BPDE-ss90mer were used as competitive probes, respectively. The two estimated binding constants are almost the same to each other, proving the rationality of the derived equation. Compared with the value ($6.36 \pm 0.54 \times 10^8\ M^{-1}$) of TMR labeled *trans*-(+)-BPDE-90mer that obtained from noncompetitive immunoassay, the obtained binding constants for the unlabeled *trans*-(+)-BPDE-90mer are a little higher. The higher binding constants may be due to the quantitative errors of BPDE-90mer by UV 260 nm. Alternatively, the hydrophobic fluorescent label in the 90mer may interact with the hydrophobic BPDE adducts in the same chain, and consequently reduce the binding affinity of the BPDE adducts to the mAb 8E11.

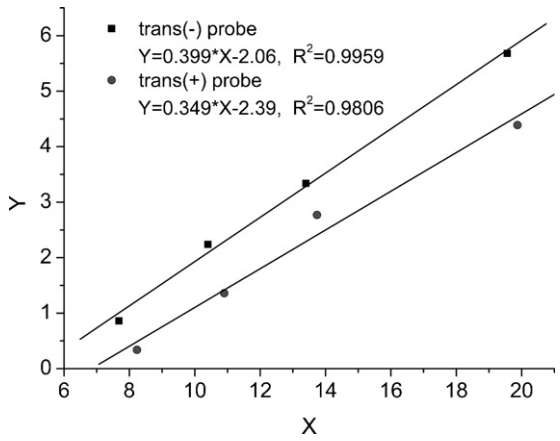


**Fig. 6.** Linear regression analysis from competitive immunoassays of BPDE adducts in genomic DNA and two BPDE-90mer probes with mAb 8E11 by Eq. (2-14). Axes *X* and *Y* are defined by Eqs. (2-15) and (2-16). The concentration of BPDE adducts in genomic DNA ranged from 6.4 to 19.1 nM while the concentrations of mAb 8E11 and TMR-BPDE-ss90mer probe were fixed at about 0.25 μg/ml and 5 nM, respectively.

The validated Eq. (2-14) was used to estimate the binding affinity of BPDE genomic DNA with mAb 8E11 in competitive immunoassays. A series of electropherograms using varying concentration of BPDE adducts in genomic DNA were shown in Fig. 5. With the increasing amount of genomic DNA, the observed probe-antibody immunocomplex (peak 2) decreases while the free probe (peak 1) increases. Fig. 6 shows the linear regression curves obtained from the data of Fig. 5 by treatment using competitive Eq. (2-14). The linear equations are $Y = 0.399 \times X - 2.06$ ($R^2 = 0.9959$) for *trans*(−) probe and $Y = 0.349 \times X - 2.39$ ($R^2 = 0.9806$) for *trans*(+) probe, respectively. The corresponding binding constants are $3.99 \pm 0.18 \times 10^8\ M^{-1}$ by *trans*(−) probe and $3.49 \pm 0.35 \times 10^8\ M^{-1}$ by *trans*(+) probe. The average binding constants of BPDE adducts in genomic DNA and mAb 8E11 ($K_b$, $3.74 \times 10^8\ M^{-1}$) is lower than

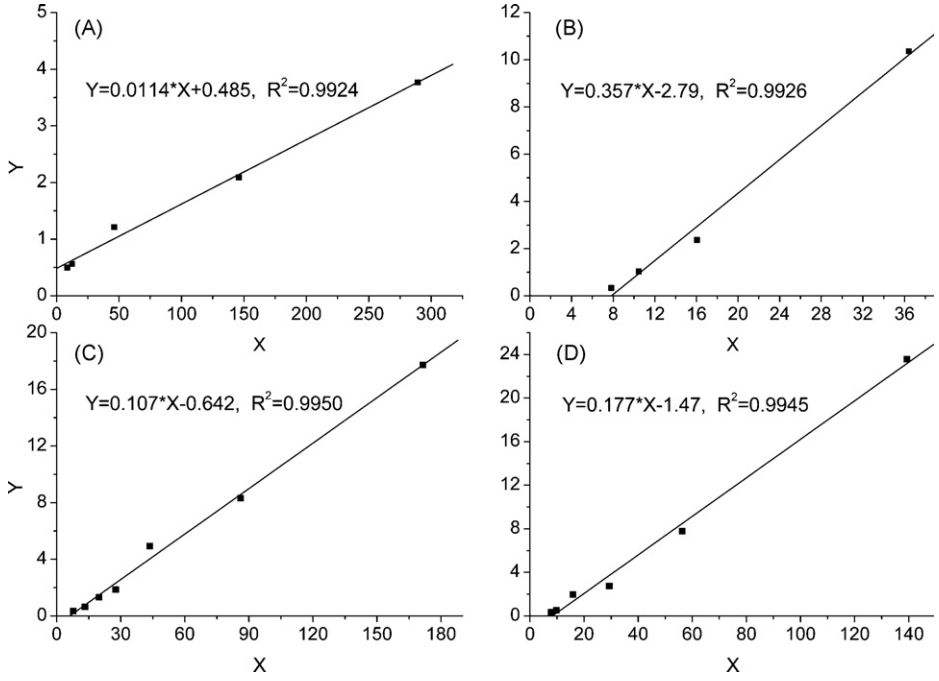


**Fig. 7.** Linear regression analysis of the data from competitive immunoassays between TMR-BPDE-90mer and four BPDE-dG stereoisomers with mAb 8E11 according to competitive Eq. (3-17). Axes *X* and *Y* are defined by Eqs. (3-18) and (3-19). A, B, C and D referred to competitors of *cis*-(−)-*anti*-BPDE-$N^2$-dG, *trans*-(+)-*anti*-BPDE-$N^2$-dG, *trans*-(−)-*anti*-BPDE-$N^2$-dG, and *cis*-(+)-*anti*-BPDE-$N^2$-dG, respectively. The concentrations of mAb 8E11 and the *trans*(−) probe were fixed at 0.25 μg/ml and 2.5 nM, respectively.

that of *trans*(−) probe ($4.52 \pm 0.52 \times 10^8\ M^{-1}$) and *trans*(+) probe ($6.36 \pm 0.54 \times 10^8\ M^{-1}$). However, the measured binding affinity is high enough for sensitive detection of BPDE-DNA adducts in genomic DNA, which is an important biomarker for human biomonitoring of carcinogenic polycyclic aromatic hydrocarbons.

### 4.3. Competitive immunoassays between TMR-BPDE-90mer and four BPDE-dG stereoisomers with mAb 8E11

Competitive CE immunoassays were also used to study the binding of four stereoisomers of *anti*-BPDE-$N^2$-dGs to mAb 8E11. The formation of the BPDE-90mer probe-antibody complex depends on the concentration of the four *anti*-BPDE-$N^2$-dGs, indicating the competitive binding of the *anti*-BPDE-$N^2$-dG and the BPDE-90mer probe to the limited binding sites of mAb 8E11 (data not shown). Unlike the binding of BPDE adducts in 90mer and genomic DNA to mAb 8E11, small *anti*-BPDE-$N^2$-dG may bind to the two sites of mAb 8E11 and form binary (1:1) and tertiary (2:1) immunocomplex. So another Eq. (3-17) was applied to estimate the binding of *anti*-BPDE-$N^2$-dG to the antibody, assuming that one antibody molecule can bind two molecules for the small antigen but only one for large BPDE-90mer.

Fig. 7 shows linear regression analysis of $Y$ with $X$ by Eq. (3-17). The $Y$ and $X$ were defined as that in the Eq. (3-17). The linear equations for four BPDE-dGs are $Y = 0.0114 \times X + 0.485$ ($R^2 = 0.9924$), $Y = 0.357 \times X - 2.79$ ($R^2 = 0.9926$), $Y = 0.107 \times X - 0.64$ ($R^2 = 0.9950$) and $Y = 0.177 \times X - 1.47$ ($R^2 = 0.9945$), respectively. According to Eq. (3-17), the corresponding binding constants are $3.57 \pm 0.22 \times 10^8\ M^{-1}$ (*trans*-(+)-BPDE-dG), $1.77 \pm 0.06 \times 10^8\ M^{-1}$ (*cis*-(+)-BPDE-dG), $1.07 \pm 0.03 \times 10^8\ M^{-1}$ (*trans*-(−)-BPDE-dG), and $1.14 \pm 0.06 \times 10^7\ M^{-1}$ (*cis*-(−)-BPDE-dG). It is obvious that the binding of the (+)-BPDE-dGs with mAb 8E11 is strongest and that of *cis*-(−)-BPDE-dG is weakest among the four stereoisomers.

## 5. Conclusions

Here we demonstrate the stereospecific binding of BPDE adducts in mononucleoside, 90mer, genomic DNA to mAb 8E11 by CE immunoassays couple with the derived equations. Noncompetitive CE immunoassays show that mAb 8E11 has a higher binding affinity with *trans*-(+)-*anti*-BPDE-90mer than *trans*-(−)-*anti*-BPDE-90mer. The binding of BPDE adduct in genomic DNA to mAb 8E11 studied by competitive CE immunoassays show that the binding affinity is high enough for mAb 8E11 to be used by immunoassay of direct detection of BPDE adduct in genomic DNA. The binding constants of four BPDE-dG stereoisomers with mAb 8E11 were also determined by competitive CE immunoassays, with an order of *trans*-(+)-BPDE-dG > *cis*-(+)-BPDE-dG > *trans*-(−)-BPDE-dG > *cis*-(−)-BPDE-dG. Our work shows that competitive CE immunoassay can be an excellent tool for the quantitative study of antigen-antibody interactions.

## Acknowledgments

This work was supported by the grants from the National Basic Research Program of China (973 program, nos. 2007CB407305 and 2010CB933500), the National Natural Science Foundation of China (nos. 20890112, 20877091, and 20921063) and the Chinese Academy of Sciences (YZ200749) to H. Wang.

## References

[1] R.A. Goldsby, T.J. Kindt, B.A. Osborne, J. Kuby, Immunology, 5th ed., W.H. Freeman & Company, New York, 2003.
[2] E. Barbar, T.M. Martin, M. Brown, M.B. Rittenberg, D.H. Peyton, Biochemistry 35 (1996) 2958.
[3] Y. Bai, C.G. Koh, M. Boreman, Y.-J. Juang, I.-C. Tang, L.J. Lee, S.-T. Yang, Langmuir 22 (2006) 9458.
[4] R.C. Ladenson, D.L. Crimmins, Y. Landt, J.H. Ladenson, Anal. Chem. 78 (2006) 4501.
[5] C.F. Grant, V. Kanda, H. Yu, D.R. Bundle, M.T. McDermott, Langmuir 24 (2008) 14125.
[6] M. Adamczyk, P.G. Mattingly, K. Shreder, Z. Yu, Bioconjugate Chem. 10 (1999) 1032.
[7] E. Kaganer, R. Pogreb, D. Davidov, I. Willner, Langmuir 15 (1999) 3920.
[8] M.R. Mazzoni, H.E. Hamm, Biochemistry 28 (1989) 9873.
[9] J.-H. Fan, E. Bochkareva, A. Bochkarev, D.M. Gray, Biochemistry 48 (2009) 1099.
[10] L. Zhu, L. Chen, H. Luo, X. Xu, Anal. Chem. 75 (2003) 6388.
[11] L.J. Brady, T. Martinez, A. Balland, Anal. Chem. 79 (2007) 9403.
[12] J.E. Butler, Methods 22 (2000) 4.
[13] C. Schou, N.H.H. Heegaard, Electrophoresis 27 (2006) 44.
[14] A.C. Moser, D.S. Hage, Electrophoresis 29 (2008) 3279.
[15] X.C. Le, J.Z. Xing, J. Lee, S.A. Leadon, M. Weinfeld, Science 280 (1998) 1066.
[16] H. Wang, M. Lu, X.C. Le, Anal. Chem. 77 (2005) 4985.
[17] N.M. Schultz, R.T. Kennedy, Anal. Chem. 65 (1993) 3161.
[18] H. Wang, J. Xing, W. Tan, M. Lam, T. Carnelley, M. Weinfeld, X.C. Le, Anal. Chem. 74 (2002) 3714.
[19] K. Shimura, B.L. Karger, Anal. Chem. 66 (1994) 9.
[20] D.H. Phillips, Nature 303 (1983) 468.
[21] W. Xue, D. Warshawsky, Toxicol. Appl. Pharmacol. 206 (2005) 73.
[22] R.F. Newbold, P. Brookes, Nature 261 (1976) 524.
[23] E. Huberman, L. Sachs, S.K. Yang, H.V. Gelboin, Proc. Natl. Acad. Sci. U. S. A 73 (1976) 607.
[24] T.J. Slaga, W.J. Bracken, G. Gleason, W. Levin, H. Yagi, D.M. Jerina, A.H. Conney, Cancer Res. 394 (1979) 67.
[25] M.K. Buening, P.G. Wislocki, W. Levin, H. Yagi, D.R. Thakker, H. Akagi, M. Koreeda, D.M. Jerina, A.H. Conney, Proc. Natl. Acad. Sci. U. S. A 11 (1978) 5358.
[26] A.W. Wood, R.L. Chang, W. Levin, H. Yagi, D.R. Thakker, D.M. Jerina, A.H. Conney, Biochem. Biophys. Res. Commun. 77 (1977) 1389.
[27] P. Brookes, M.R. Osborne, Carcinogenesis 3 (1982) 1223.
[28] J.A. Burgess, C.W. Stevens, W.E. Fahl, Cancer Res. 45 (1985) 4257.
[29] S. Hoare, Y. Zou, V. Purohit, R. Krishnasamy, M. Skorvaga, B. Van Houten, N.E. Geacintov, A.K. Basu, Biochemistry 39 (2000) 12252.
[30] Y. Zou, S.M. Shell, C.D. Utzat, C. Luo, Z. Yang, N.E. Geacintov, A.K. Basu, Biochemistry 42 (2003) 12654.
[31] Y. Pommier, G. Kohlhagen, P. Pourquier, J.M. Sayer, H. Kroth, D.M. Jerina, Proc. Natl. Acad. Sci. U. S. A. 97 (2000) 2040.
[32] N. Suzuki, E. Ohashi, A. Kolbanovskiy, N.E. Geacintov, A.P. Grollman, H. Ohmori, S. Shibutani, Biochemistry 41 (2002) 6100.
[33] D. Chiapperino, H. Kroth, I.H. Kramarczuk, J.M. Sayer, C. Masutani, F. Hanaoka, D.M. Jerina, A.M. Cheh, J. Biol. Chem. 277 (2002) 11765.
[34] O. Rechkoblit, Y. Zhang, D. Guo, Z. Wang, S. Amin, J. Krzeminsky, N. Louneva, N.E. Geacintov, J. Biol. Chem. 277 (2002) 30488.
[35] R.M. Santella, C.D. Lin, W.L. Cleveland, I.B. Weinstein, Carcinogenesis 5 (1984) 373.
[36] T.J. Carnelley, S. Barker, H. Wang, W.G. Tan, M. Weinfeld, X.C. Le, Chem. Res. Toxicol. 14 (2001) 1513.
[37] T.M. Hsu, T.M. Liu, S. Amin, N.E. Geacintov, R.M. Santella, Carcinogenesis 16 (1995) 2263.
[38] S. Venkatachalam, A.A. Wani, Carcinogenesis 15 (1994) 565.
[39] F.J. Van Schooten, E. Kriek, M.-J.S.T. Steenwinkel, H.P.J.M. Noteborn, M.J.X. Hillebrand, F.E. Van Leeuwen, Carcinogenesis 8 (1987) 1263.
[40] R.A. Baan, P.T.M. van den Berg, W.P. Watson, R.J. Smith, Toxicol. Environ. Chem. 16 (1988) 325.
[41] W.G. Tan, T.J. Carnelley, P. Murphy, H. Wang, J. Lee, S. Barker, M. Weinfeld, X.C. Le, J. Chromatogr. A 924 (2001) 377.
[42] H. Wang, M. Lu, N. Mei, J. Lee, M. Weinfeld, X.C. Le, Anal. Chim. Acta 500 (2003) 13.
[43] Z. Wang, M. Lu, X. Wang, R. Yin, Y. Song, X.C. Le, H. Wang, Anal. Chem. 81 (2009) 10285.
[44] C. Wang, F. Feng, Z. Wang, T. Li, X.C. Le, H. Wang, Chem. Res. Toxicol. 22 (2009) 676.
[45] F. Feng, J. Yin, M. Song, H. Wang, J. Chromatogr. A 1183 (2008) 119.
[46] F. Feng, X. Wang, H. Yuan, H. Wang, J. Chromatogr. B 877 (2009) 2104.
[47] Z. Wang, C. Wang, J. Yin, T. Li, M. Song, M. Lu, H. Wang, Electrophoresis 29 (2008) 4454.
[48] H. Wang, M. Lu, M. Weinfeld, X.C. Le, Anal. Chem. 75 (2003) 247.